

Extracting IP information from AEM data to improve the hydrogeological interpretation

Viezzoli Andrea*

Aarhus Geophysics Aps
C.F.Møllers Allé 4,
DK-8000 Aarhus C, DK
av@aarhusgeo.com

Vlad Kaminski

Aarhus Geophysics Aps
C.F.Møllers Allé 4,
DK-8000 Aarhus C, DK
vlad.kaminski@aarhusgeo.com

Nicholas Ebner

Newexco Services
15 Joel Tce, East Perth
WA
nick@newexco.com.au

Antonio Menghini

Aarhus Geofisica Srl
Via Giuntini 13
56023, Pisa, Italy
am@aarhusgeo.com

SUMMARY

IP measurements in airborne EM data have not been previously considered for mapping groundwater distribution. IP modelling can be applied to discriminate between co-existing salty aquifers (conductive and non-chargeable) and extensive clay layers (conductive and chargeable); typical in both coastal areas and regions affected by dry-land salinity. The current case study presents the field results from a gold and metal project that had a hydrogeological mapping component to it in central Western Australia. Accounting for IP signal in the forward response was necessary to fit the data in localised areas, which were then interpreted as clay filled (conductive and chargeable) palaeochannels. The synthetic experiments that followed confirm that in favourable conditions, clay derived IP signal can affect the measured AEM response. Conversely, IP information can be recovered from these data, providing an extra physical parameter of value to the hydrogeological interpretation.

Key words: Airborne EM, IP, inversion, Hydrogeology, Chargeability, Clays, Salt water.

INTRODUCTION

The relevance of IP effects in AEM data is presently recognised both by industry and academia. Despite ongoing discussions concerning the depth at which chargeability can affect AEM data and be subsequently recovered; the consensus is that it can have a role in mineral exploration. In this paper we focus on an unexpected hydrogeological application, potentially very relevant to places affected by dryland salinity, especially Australia. This concerns the possibility of distinguishing between salty aquifers and clays with airborne IP. The rationale is that both clays and salty aquifers are conductive, but only clay is chargeable. Ground IP has been used with some success to this effect. Typically for EM, where the sensor is airborne, signal associated with chargeable clays is generally expected to be too small to be measured and recoverable. Analysis of the Thaduna VTEM dataset from central Western Australia was subsequently undertaken (Figure 1). The survey, recorded in March 2010, shows indications of a regolith derived chargeable signal which impacts the derived resistivities and geometries when the IP is not considered. A comparison with synthetics studies was initiated.

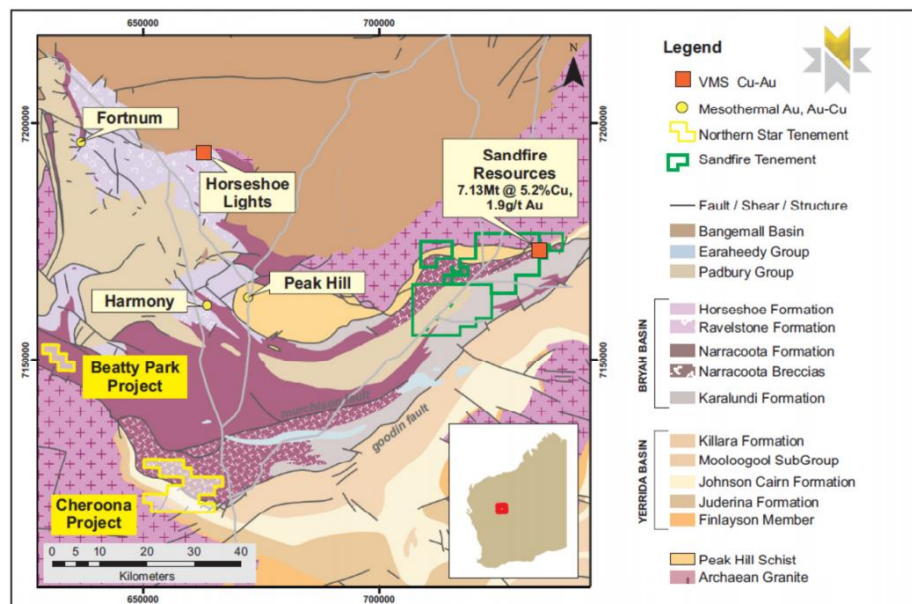


Figure 1: Location of Sandfire project (adapted from: <http://www.sandfire.com.au/>)

METHOD AND RESULTS

The VTEM dataset was analysed for two purposes: 1) modelling the regolith profile to improve planning and interpretation of soil geochemical surveys; and 2) mapping bedrock geological structures in areas where interpreted maghaemite in palaeochannels obscures the otherwise valuable magnetic data used for this purpose. Note that no study has confirmed maghaemite as the direct source.

The EM data was first processed to increase the S/N ratio and eliminate artefacts, before employing a Spatially Constrained Inversion (SCI) (Viezzoli et al., 2008). No IP effects were expected, nor were they clearly visible in the data, so the modelling was carried out using the standard, non-dispersive resistivity. In general, the results were satisfactory, with adequate mapping of known structural features, and good correlation with ancillary structural information derived from the magnetic vertical derivative in areas where the maghaemite response was negligible (Figure 2a).

However the spatial distribution of the misfit, which resembles the known palaeochannels (Figure 2b) demanded a review of the data. The possibility of higher data misfit being related to 3D effects in the quasi 3D SCI inversion was disregarded. The higher misfit coincides with the widest portions of the palaeochannels (approximately 500m), well beyond the expected footprint of the VTEM system at that shallow depth. Attention was then turned to the presence of IP signal in the data. In very limited parts of the survey the late time voltages show negative values, whereas in correspondence to some of the misfit maxima, observed transients show anomalously fast decays. Both anomalies can be associated with a distorted decay, as would be expected in case of IP effects. The data were therefore reprocessed and reinverted using the Cole-Cole model (and SCI approach) in AarhusInv inversion code, modified according to Fiandaca et al. (2012). The code solves for Complex Impedance (dispersive resistivity), using the model of Cole-Cole (1941) and provided simultaneous estimation of ρ , c , m and τ . This resulted in an improved data fit (Figure 2d), which was no longer showing patterns consistent with palaeochannels geometries. The resistivity models (Figure 2c) show improved contrast in 2d. The palaeochannels exhibit chargeability maxima (Figure 2e). The palaeochannels, modelled as conductive and chargeable, implies they are filled with clay-like fine grained material, rather than being a sandy aquifer, filled with non-chargeable salty groundwater. The client has confirmed that palaeochannels in the area are dominated by fine grained clay sediments. Generally, the geological interpretation of this setting is that of a low energy cannibalistic system, with clays from in-situ lateritic weathering of the regolith profile being eroded and redeposited in the palaeochannels. No groundwater measurements or geophysical log data were available within the palaeochannel features; however, there is a strong suggestion from nearby sites, including the DeGrussa Copper Mine, that the groundwater in the area is potable. Maghaemite is also present in the area and is the likely cause of the magnetic and relatively conductive features at the edges of the palaeochannels. The presence of maghaemite gravel at the base of the palaeochannels is also possible, but their expected resistive nature would not allow discrimination within bedrock.

Furthermore, we realise that invoking the IP model in an area where clays are assumed the only source of IP signal, requires more thorough numerical analysis. We therefore generated a number of synthetic examples. We simulated a sequence of full-waveform VTEM data sets, which are contaminated with noise and inverted in order to study how well certain targets can be recovered. In the forward model, a long-pulse 2015 VTEM full waveform was considered. In the model presented here, several synthetic buried valleys are placed beneath an overburden and assigned high electrical conductivity and varying chargeability values from non-chargeable, to moderately chargeable and finally, very chargeable. The ability to discriminate between layers of variable chargeability beneath overburden is studied. The results suggest that in some cases the IP effect was indeed negligible in both data and model space. In others, however, it was measureable. We present one of those cases (Figure 3). The 5 valleys shown are filled with a combination of resistivity and chargeability values that represent a gradual transition from salty aquifers to clay filled aquitards. Note the chargeability (m_0) values range from 0 to 300 mV/V.

The recovered models, associated to satisfying data misfit, are in good agreement with the true models, both in the resistivity and chargeability domains. The 2 parameters display some coupling (e.g., valley 1), but in general provide complementary diagnostic results. Both the forward response (not shown) and the inverted models are indicative of the possibility resolving the clay versus salt aquifers targets, not just for the highest chargeabilities, but also for moderate values of m_0 (30 to 100 mV/V).

Notice also that comparing between chargeabilities obtained from ground galvanic IP surveys and TDEM measurements (ground or airborne) should be done with caution, given their very different frequency ranges. The evidence above prove: a) that IP effects can be the cause of the anomalous response measured within some of the paleochannels in this AEM case study, and b) that they can be accounted for.

CONCLUSIONS

Perhaps surprisingly AEM data are found to display, in some cases, IP effects that can be attributed to clays. Both real and synthetic data support this conclusion. In the field example, IP effects in VTEM data help the hydrogeological interpretation, providing an extra physical parameter that enables clays to be discriminated from saline aquifers.

The results and evidence uncovered in this case study could have relevant applications to hydrogeological mapping with AEM in areas affected by salinity.

ACKNOWLEDGMENTS

We would like to thank Sandfire Resources for permission to present the data and their geological feedback.

REFERENCES

- Cole, K. S., and Cole, R. H., 1941, Dispersion and absorption in dielectrics: *Journal of Chemical Physics*, 9-4, 341–351.
- Fiandaca, G., Ramm, J., Binley, A., Gazoty, A., Christiansen, A. V., and Auken, E., 2012, Resolving spectral information from time domain induced polarization data through 2-D inversion: *Geophysical Journal International*.

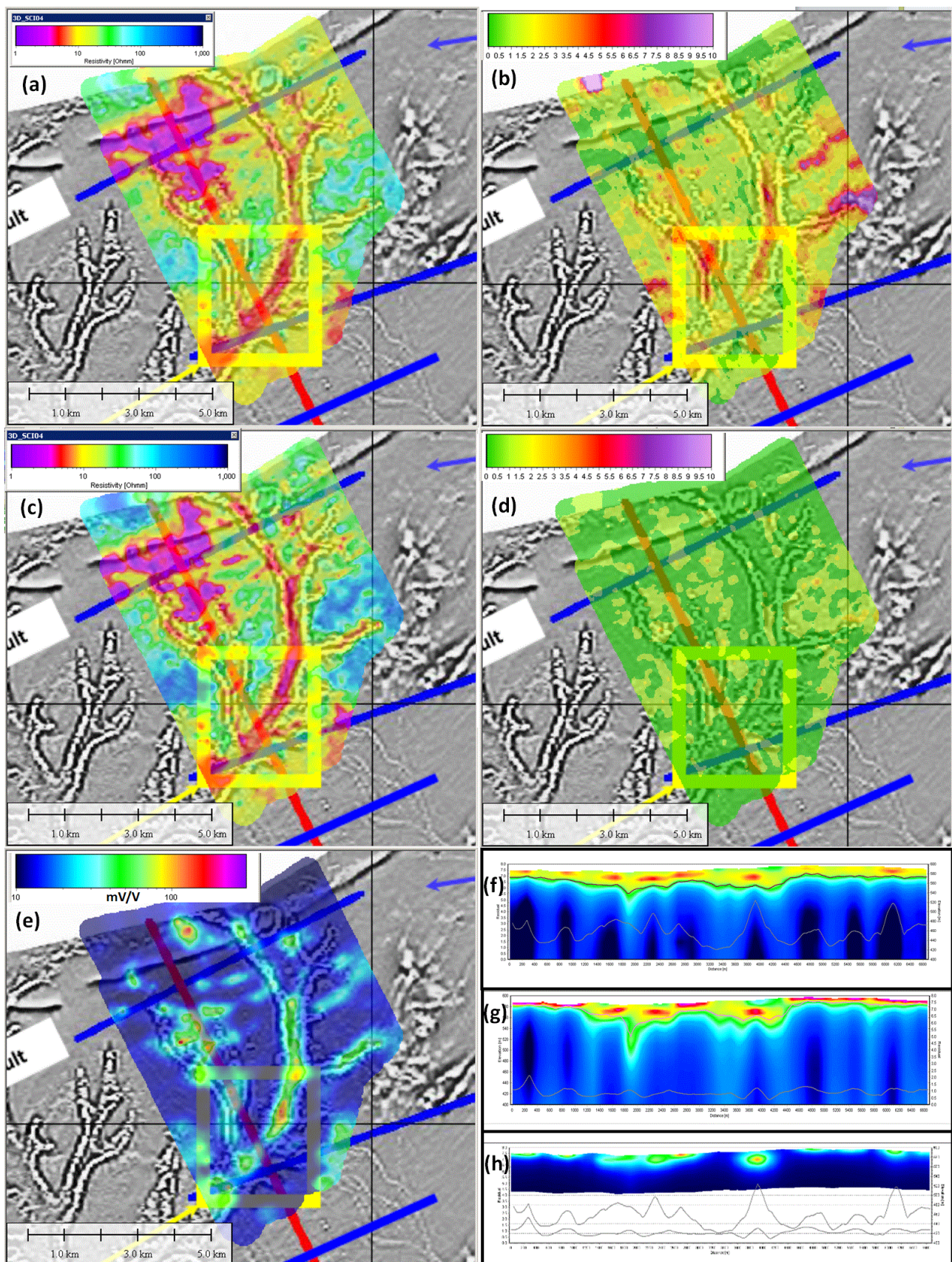


Figure 2: Cole-Cole parameters recovered by SCI inversions. (a) Resistivity without modelling of IP effect at 20-30 m depth interval. (b) Data misfit, associated with “no-IP” modelling. (c) Recovered electrical resistivity with modelling of IP effect at 20-30 m depth interval. (d) Data misfit associated with IP modelling. (e) Recovered chargeability section at 20-30 m interval. (f) Resistivity cross-section (“no-IP” model). (g) Resistivity cross-section (IP model). (h) Chargeability cross-section.

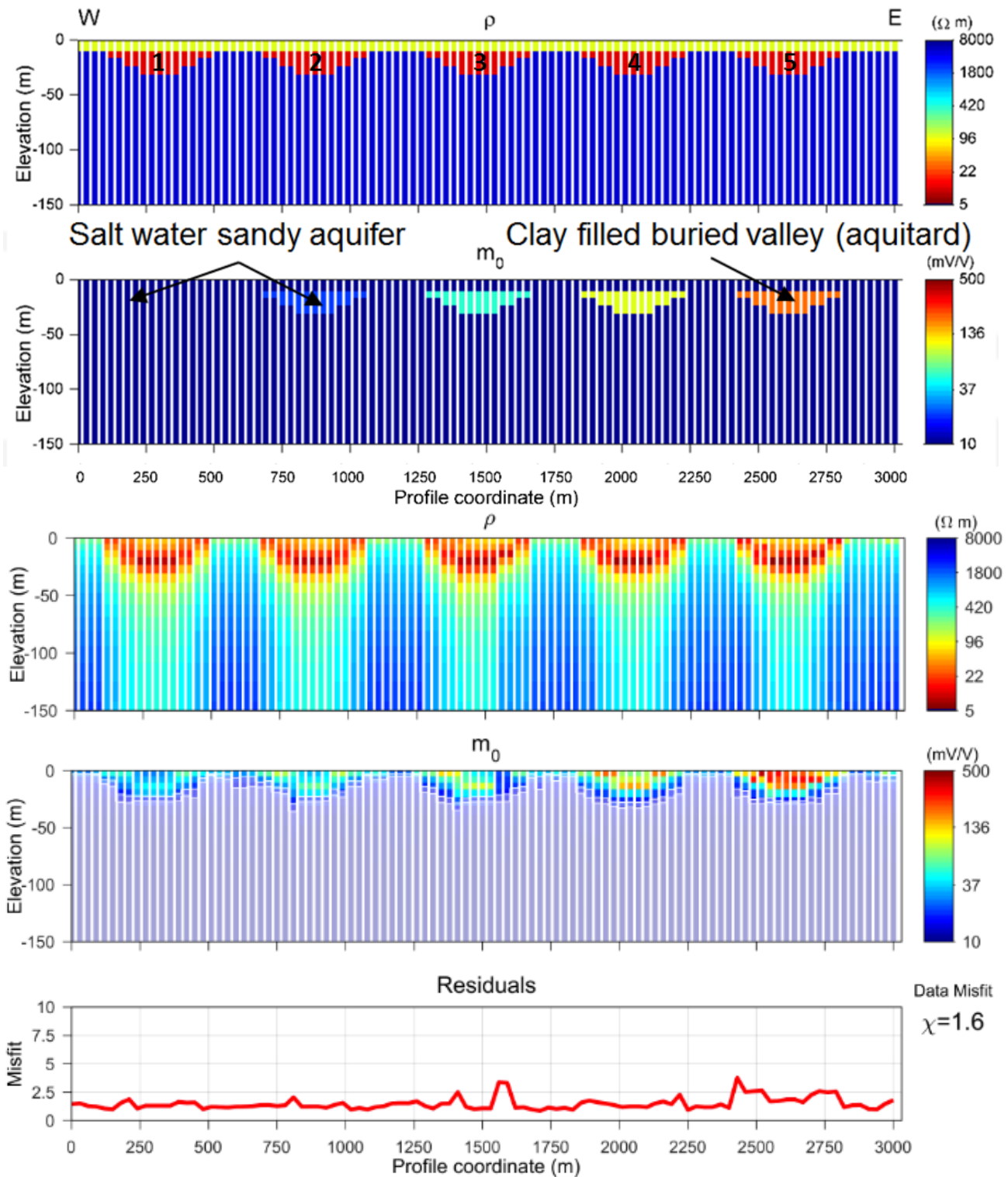


Figure 3: Synthetic experiment to identify whether IP effects in AEM data can differentiate between clays and salty aquifers. True models presented in two uppermost panels; recovered Cole-Cole parameters are shown underneath. Data misfit is at the bottom.